The Finite-Element Solution of Laminar Combined Convection from Two Horizontal Cylinders in Tandem Arrangement

A finite-element method is used to solve the full Navier-Stokes and energy equations for the problem of laminar combined convection from two horizontal cylinders in tandem arrangement. From comparisons with the previous theoretical and experimental results of a single-cylinder situation, it is found that the behaviors flow and heat transfer in the upstream cylinder are close to those in a single-cylinder, but this is not the case for the downstream cylinder.

King-Leung Wong
Cha'o-Kuang Chen
Department of Mechanical Engineering
National Cheng-Kung University
Tainan, Republic of China

SCOPE

Heat transfer from horizontal circular cylinders has been the subject of numerous analytical and experimental investigations from the standpoint of pure free convection or pure forced convection. In the situation where the velocity is small and the temperature difference between the surface and the ambient fluid is large, predictions of the flow and heat transfer characteristics in the combined convection regime are of practical interest. Previous investigations of combined convection from horizontal cylinders were restricted to a single-cylinder situation.

The behaviors of flow for circular cylinders in tandem arrangement have been studied widely. But the problem of laminar combined convection from two circular cylinders in tandem arrangement has not been reported. In the present work, the problems of laminar combined convection from two cylinders of the same diameter in tandem arrangement with spacing between the cylinders at a value of two diameters, is solved by a finite-element method. In order to find the differences in behavior of flow and heat transfer between the situations of two cylinders and a single cylinder, numerical results of the upstream and downstream cylinders are compared with the previous theoretical and experimental results for a single cylinder.

CONCLUSIONS AND SIGNIFICANCE

The finite-element method is based on the full Navier-Stokes and energy equations. Numerical results are obtained for gases having a Prandtl number of 0.7 over the entire surfaces of two cylinders, including the zones beyond the separation point. It is found that the parameter Gr/Re^2 on the increases for the surface shear stress, the Nusselt number, and the shift of separation point are significant, especially for the downstream cylinder. From comparisons between the results of the two cylinders in tandem arrangement and the results of Dennis and Chang (1970), Badr (1984), and Jackson and Yen (1971) for a single-cylinder situation, it is found that the behaviors of flow and heat transfer in the upstream cylinder are close to those of a single cylinder, but this is not the case for the downstream cylinder. The results are of interest and may be of some importance in heat exchange problems.

Correspondence concerning this paper should be directed to C. K. Chen.

Introduction

Combined forced and natural convection heat transfer from horizontal cylinders continues to be an important problem, due to its fundamental nature as well as its many related engineering applications. For the single-cylinder problem, a good number of experimental and theoretical investigations have been carried out in the past. Joshi and Sukhatme (1971), Sparrow and Lee (1976), and Merkin (1976) presented work based on the boundary layer equations. In their studies the velocity distribution outside the boundary layer was assumed to be exactly the same as that of potential flow. Under that assumption, their studies were limited to the region from the forward stagnation point up to the point of separation only. Accordingly, the average Nusselt number over the cylinder surface could not be obtained. Dennis and Chang (1970) presented the numerical solutions for steady flow past a circular cylinder at Reynolds numbers up to 100. Lately, Badr (1984) has presented a numerical method to deal with the problem of combined convection from a horizontal cylinder. The method is based on the solution of the full Navier-Stokes and energy equations. Numerous experimental investigations were carried out to study the effect of various parameters on the rate of heat transfer from a horizontal cylinder. The first comprehensive experimental work on the single-cylinder problem was carried out by Hatton et al. (1970), who studied combined convection from a horizontal cylinder up to $Re = 50$ and Rayleigh number, $Ra = 10$. Oosthuizen and Madan (1970) considered the problem of a cylinder for parallel flow in the range of $100 < Re < 3{,}000$ and Grashof number $25{,}000 < Gr < 300{,}000$. Based on their experimental data, a correlation for the average Nusselt number was obtained. An alternative correlation of the same data obtained by Jackson and Yen (1971) was found to fit the data better, especially at higher values of Gr/Re^2.

The time-mean surface pressure and the vortex-shedding characteristics of two circular cylinders of the same diameter in tandem arrangement have been extensively studied for many years. For example, Igarashi (1980) and Arie et al. (1983) presented work on flow characteristics around two horizontal cylinders in tandem arrangement.

Investigations of combined convection from the horizontal cylinder have been restricted to a single-cylinder situation. The problem of combined convection from two cylinders in tandem arrangement has received relatively little attention. In the present work, the problem of combined convection from two cylinders of the same diameter in tandem arrangement with the spacing between the cylinder centers at a value of two diameters, is solved by a finite-element method. The method is based on the solution of the full Navier-Stokes and energy equations. The numerical results are obtained for gases having a $Pr = 0.7$ over the entire surfaces of two cylinders, including the zones beyond the separation point.

Problem Statement

Consider two isothermal horizontal cylinders of radius Ro and temperature Tw, placed in a uniform free stream of temperature $T\infty$ and velocity $u\infty$ in tandem arrangement, with the spacing between the cylinder centers at a value of two diameters. The free stream is directed opposite to the direction of gravitational acceleration. The cylinders are considered to be long enough so that the end effects can be neglected, and accordingly the flow field can be assumed to be two-dimensional. Using Cartesian coordinates with x and y axes, the calculated flow domain, boundary conditions, and coordinates of the flow field are shown in Figure 1.

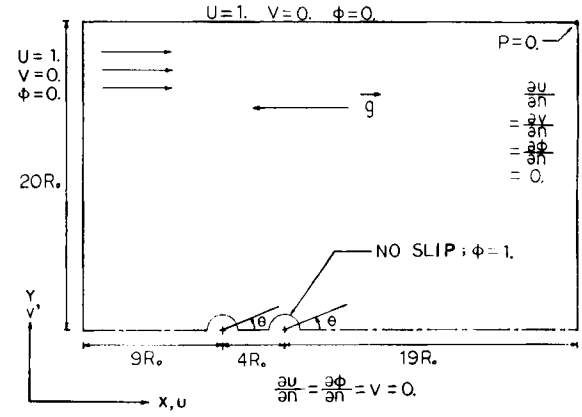

Figure 1. Calculated flow domain, boundary conditions, and coordinates.

The temperature difference $\Delta T(=Tw - T\infty)$ is assumed to have a neglegible effect on the fluid properties except for the buoyancy force in the momentum equation, and the fluid is incompressible. Consider the line $\theta = 0°$ to be the radius through the rearmost cylinder surface viewed from the upstream direction. The dimensionless governing equations can be written as follows:

Continuity equation:

$$\frac{\partial u}{\partial x} + \frac{\partial v}{\partial y} = 0 \tag{1}$$

Momentum equations:

$$u\frac{\partial u}{\partial x} + v\frac{\partial u}{\partial y} = -\frac{\partial p}{\partial x} + \frac{1}{Re}\left(\frac{\partial^2 u}{\partial x^2} + \frac{\partial^2 u}{\partial y^2}\right) + \frac{Gr}{Re^2}\phi \tag{2}$$

$$u\frac{\partial u}{\partial x} + v\frac{\partial v}{\partial y} = -\frac{\partial p}{\partial y} + \frac{1}{Re}\left(\frac{\partial^2 v}{\partial x^2} + \frac{\partial^2 v}{\partial y^2}\right) \tag{3}$$

Energy equation:

$$u\frac{\partial \phi}{\partial x} + v\frac{\partial \phi}{\partial y} = \frac{1}{Pe}\left(\frac{\partial^2 \phi}{\partial x^2} + \frac{\partial^2 \phi}{\partial y^2}\right) \tag{4}$$

where

$$u = \frac{u^*}{u\infty}, \quad v = \frac{v^*}{u\infty}, \quad \phi = \frac{T - T\infty}{Tw - T\infty}, \quad p = \frac{p^* - p\infty}{\rho u^2 \infty}$$

$$x = \frac{x^*}{2Ro}, \quad y = \frac{y^*}{2Ro}, \quad Re = \frac{2u\infty Ro}{\nu}, \quad Pr = \frac{\mu c}{k}$$

$$Pe = P_r Re, \quad Gr = \frac{8g\beta\,(Tw - T\infty)\,Ro^3}{\nu^2}$$

Finite-Element Method

Owing to the symmetry of the flow field, only one-half of the total domain of flow needs to be considered. The calculated flow domain is discretized into 111 elements, as shown in Figure 2. All of the elements are isoparametric quadrilaterals containing eight nodes, one at each corner and one at the midpoint of each

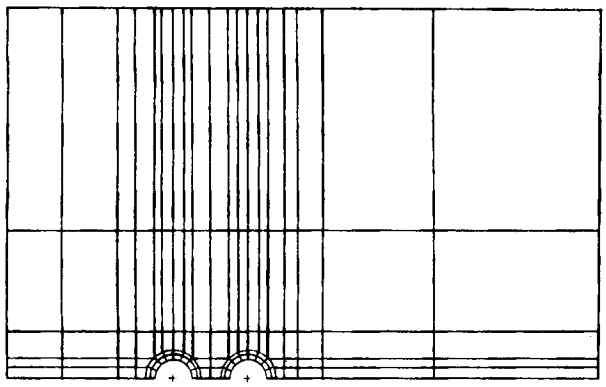

Figure 2. Element discretization of calculated flow domain.

side. All eight nodes are associated with velocities and temperature, but only the corner nodes are associated with pressure. Following an accepted practice mentioned by Taylor and Hughes (1981) depicting the variation in pressure by shape functions, $M\ell$, of one order lower than those, Ni, for defining the velocity and temperature,

$$\left.\begin{aligned} u &= \sum_{j=1}^{8} N_j u_j, \qquad v = \sum_{j=1}^{8} N_j v_j \\ \phi &= \sum_{j=1}^{8} N_j \phi_j, \qquad p = \sum_{l=1}^{4} M\ell p\ell \end{aligned}\right\} \tag{5}$$

Employing the Galerkin weighted residual approach, Eq. 1 becomes

$$\sum_{1}^{n^e} \int_{A^e} M_i \left(\frac{\partial N_j}{\partial x} u_j + \frac{\partial N_j}{\partial y} v_j \right) dA^e = 0 \tag{6}$$

where n^e = total element number (111 for the present work),
$i = 1, 2, 3, 4; \quad j = 1, 2, \ldots, 8$
A^e = area of single element

Equation 2 becomes:

$$\sum_{1}^{n^e} \int_{A^e} \left[N_i N_k u_k \frac{\partial N_j}{\partial x} u_j + N_i N_k v_k \frac{\partial N_j}{\partial y} u_j + N_i \frac{\partial M\ell}{\partial x} p\ell + \frac{1}{Re} \left(\frac{\partial N_i}{\partial x} \frac{\partial N_j}{\partial x} u_j + \frac{\partial N_i}{\partial y} \frac{\partial N_j}{\partial y} u_j \right) - \frac{Gr}{Re^2} N_i N_j \phi_j \right] dA^e - \int_{\Gamma_1} \frac{1}{Re} N_i \frac{\partial N_j}{\partial n} u_j \, d\Gamma - \int_{\Gamma_2} \frac{1}{Re} N_i \left(\frac{\partial u}{\partial n} \right) d\Gamma = 0 \tag{7}$$

Equation 3 becomes:

$$\sum_{1}^{n^e} \int_{A^e} \left[N_i N_k u_k \frac{\partial N_j}{\partial x} v_j + N_i N_k v_k \frac{\partial N_j}{\partial y} v_j + N_i \frac{\partial M\ell}{\partial y} p\ell + \frac{1}{Re} \left(\frac{\partial N_i}{\partial x} \frac{\partial N_j}{\partial x} v_j + \frac{\partial N_i}{\partial y} \frac{\partial N_j}{\partial y} v_j \right) \right] dA^e - \int_{\Gamma_1} \frac{1}{Re} N_i \left(\frac{\partial N_j}{\partial n} \right) v_j \, d\Gamma - \int_{\Gamma_2} \frac{1}{Re} N_i \left(\frac{\partial v}{\partial n} \right) d\Gamma = 0 \tag{8}$$

And Eq. 4 becomes:

$$\sum_{1}^{n^e} \int_{A^e} \left[N_i N_k u_k \frac{\partial N_j}{\partial x} \phi_j + N_i N_k v_k \frac{\partial N_j}{\partial y} \phi_j + \frac{1}{Pe} \left(\frac{\partial N_i}{\partial x} \frac{\partial N_j}{\partial x} \phi_j + \frac{\partial N_i}{\partial y} \frac{\partial N_j}{\partial y} \phi_j \right) \right] dA^e + \int_{\Gamma_1} \frac{1}{Pe} N_i \frac{\partial N_j}{\partial n} \phi_j \, d\Gamma - \int_{\Gamma_2} \frac{1}{Pe} N_i \left(\frac{\partial \phi}{\partial n} \right) d\Gamma = 0 \tag{9}$$

where

$$i, j, k = 1, 2, \ldots, 8; \qquad \ell = 1, 2, 3, 4$$

Combining Eqs. 7, 8, and 9 into the form of assembled matrix equations

$$\tilde{\mathbf{A}} \tilde{\lambda} = \tilde{\mathbf{B}} \tag{10}$$

where the vector of primitive variables $\tilde{\lambda}$ is

$$\lambda_j = \begin{bmatrix} u_j \\ p_j \\ v_j \\ \phi_j \end{bmatrix} \tag{11}$$

Each coefficient in the matrix $\tilde{\mathbf{A}}$ has the form

$$a_{ij} = \sum_{1}^{n^e} \int_{A^e} \begin{bmatrix} C_{11} & C_{12} & C_{13} & C_{14} \\ C_{21} & C_{22} & C_{23} & C_{24} \\ C_{31} & C_{32} & C_{33} & C_{34} \\ C_{41} & C_{42} & C_{43} & C_{44} \end{bmatrix} dA^e - \int_{\Gamma_1} \begin{bmatrix} \frac{1}{\mathrm{Re}} N_i \frac{\partial N_j}{\partial n} & 0 & 0 & 0 \\ 0 & 0 & 0 & 0 \\ 0 & 0 & \frac{1}{\mathrm{Re}} N_i \frac{\partial N_j}{\partial n} & 0 \\ 0 & 0 & 0 & \frac{1}{\mathrm{Pe}} N_i \frac{\partial N_j}{\partial n} \end{bmatrix} d\Gamma \tag{12}$$

where

$$C_{11} = N_i N_k u_k \frac{\partial N_j}{\partial x} + N_i N_k v_k \frac{\partial N_j}{\partial y} + \frac{1}{Re} \left(\frac{\partial N_i}{\partial x} \frac{\partial N_j}{\partial x} + \frac{\partial N_i}{\partial y} \frac{\partial N_j}{\partial y} \right)$$

$$C_{12} = N_i \frac{\partial M\ell}{\partial x}, \; C_{13} = 0, \; C_{14} = \frac{-\mathrm{Gr}}{Re^2} N_j, \; C_{21} = M_i \frac{\partial N_j}{\partial x}, \; C_{22} = 0$$

$$C_{23} = M_i \frac{\partial N_j}{\partial y}, \; C_{24} = 0, \; C_{31} = 0, \; C_{32} = N_i \frac{\partial M\ell}{\partial y}, \; C_{33} = C_{11}$$

$$C_{34} = 0, \; C_{41} = 0, \; C_{42} = 0, \; C_{43} = 0$$

$$C_{44} = N_i N_k u_k \frac{\partial N_j}{\partial x} + N_i N_k v_k \frac{\partial N_j}{\partial y} + \frac{1}{Pe}\left(\frac{\partial N_i}{\partial x}\frac{\partial N_j}{\partial x} + \frac{\partial N_j}{\partial y}\frac{\partial N_j}{\partial y}\right)$$

Each coefficient in the matrix $\tilde{\mathbf{B}}$ has the form

$$b_i = \int_{\Gamma_2} \begin{bmatrix} b_1 \\ b_2 \\ b_3 \\ b_4 \end{bmatrix} d\Gamma \tag{13}$$

where

$$b_1 = \frac{1}{Re} N_i \left(\frac{\partial u}{\partial n}\right), \; b_2 = 0,$$

$$b_3 = \frac{1}{Re} N_i \left(\frac{\partial v}{\partial n}\right), \; b_4 = \frac{1}{Pe} N_i \left(\frac{\partial \phi}{\partial n}\right)$$

Numerical solution

There is a standard procedure in evaluating the above integrations; it is mentioned in a number of technical books and papers in the field of finite-element analysis, such as Taylor and Hughes (1981). The procedure involves normalization of the coordinates and use of the Gauss-Legendre quadrature scheme. In the work, the 3 × 3 and 3 × 1 Gaussian integration sampling point schemes are used for the surface and line integrals, respectively. The resultant nonlinear asymmetric matrix equations are solved by the frontal width method introduced by Irons (1970) and Hood (1976) and a suitable iterative process.

Physical parameters

Nusselt Number. From the definition of the convective heat transfer coefficient

$$-k \nabla^* T = h(T_w - T_\infty) \qquad \text{or} \quad -k \frac{1}{2R_o} \nabla \phi = h$$

The local Nusselt number can be written as

$$Nu = \frac{2hR_o}{k} = -\nabla \phi = \frac{\partial N_j}{\partial n} \phi_j \tag{14}$$

where

$$j = 1, 2, \text{----}, 8$$

The average Nusselt number is defined as

$$\overline{N_u} = \frac{1}{\pi} \int_0^\pi N_u d\theta \tag{15}$$

Shear Stress. The shear stress for a Newtonian fluid is given by

$$\tau_w^* = \mu \frac{\partial u_t^*}{\partial_n^*} = \frac{\mu u_\infty}{2R_o} \frac{\partial u_t}{\partial n}$$

where $\partial u_t / \partial n$ denotes the dimensionless gradient of tangential velocity in the direction normal to the cylinder surface. Thus the dimensionsless shear stress is

$$\tau_w = \frac{\tau_w^*}{\rho u_\infty^2} = \frac{\mu}{2\rho u_\infty R_o} \frac{\partial u_t}{\partial n} = \frac{1}{Re} \frac{\partial u_t}{\partial n}$$
$$= \frac{1}{Re} \frac{\partial N_j}{\partial n} (u_j \sin\theta - v_j \cos\theta) \tag{16}$$

Total Friction Drag Coefficient. The definition is given as

$$C_f = \frac{1}{\partial R_o^2} \int_0^\pi \tau_w \sin\theta \, d\theta \tag{17}$$

Results and Discussions

The problem of laminar combined convection from two isothermal hot horizontal cylinders in tandem arrangement with a spacing between the centers of the cylinders at the value of two diameters, is studied for the parallel flow regime at Re = 5, 10, 20, 40, 60, and 100 for different values of Gr when Pr = 0.7. The results of average Nusselt number $\overline{Nu}$, the angle of separation θs, and total friction drag coefficient Cf are listed in Table 1.

From Table 1 it can be seen that for the single-cylinder situation and pure forced convection cases (i.e., Gr = 0), the greater the Re, the greater the $\overline{Nu}$ and θs, but the smaller the Cf; and at the same Re, the greater the Gr, the greater $\overline{Nu}$ and Cf, but the smaller the θs. The increasing Gr tends to delay the flow of separation for the single-cylinder situation. Accordingly, the location of the point of separation depends on Re as well as Gr. Badr (1984) concluded that there exists no circulation in the wake for $Re \leq 5$ for the single-cylinder situation but not for both cylinders in a tandem arrangement. From Table 1 it can be seen that for pure forced convection cases the flow separation of the upstream cylinder occurs earlier than that of the single cylinder for all the cases. Thus, the shift of an earlier separation of the upstream cylinder is due to the effect of the downstream cylinder. In combined convection cases, it is found that the increasing Gr tends to delay the flow separation for the upstream cylinder and shifts the location of the front flow separation to a greater angle as well as the rear flow separation to a smaller angle for the downstream cylinder. It can be seen from Table 1 that in the range of Re considered, the location of the separation point depends on Re as well as Gr for both cylinders. When $Gr/Re^2 \geq 1.0$, there exists no flow of separation in the range of Re considered for the single-cylinder situation, but not for both the cylinders in tandem arrangement. We cannot conclude that at a certain value of Gr/Re^2 for the Re considered there exists no flow separation for both cylinders, because Table 1 shows that the greater the Re, the greater the Gr/Re^2 for nonexistence of flow separation. For example, when $Gr/Re^2 \geq 1.0$, there is no flow separation for both cylinders for the case at Re = 20 but not for the cases at Re = 40 and 60.

The dimensionless surface shear stress distributions at Re = 20 and 40 for different values of Gr are given in Figures 3 and 4, respectively. It is clear from Eq. 16 that $Re\tau_w = 2\partial U_t / \partial n$. When $Re\tau_w = 0$, it denotes the point at which the flow of separation does occur. Thus, the angles of separation can be found at the intersection points on the line $Re\tau_w = 0$ in Figures 3 and 4. It can also be seen in these figures that the increasing Gr tends to create a significant increase in the surface shear stress, especially

Table 1. Summary of Predictions

Re	Gr	Gr/Re^2	$\overline{Nu}_1$*	$\overline{Nu}_2$*	θs_1,°	θs_2,°	Cf_1	Cf_2
5	0	0	1.355	0.686	29.31	156.36, 0	4.034	1.840
			(1.450)**			(0)		
			[1.496]			[0]	[4.461]	
10	0	0	1.827	0.893	36.34	152.83, 0	2.611	1.084
			[1.959]			[28.95]	[2.831]	
20	0	0	2.449	1.205	46.01	145.54, 29.74	1.706	0.616
			(2.540)			(43.13)	(—)	
			[2.580]			[43.58]	[1.813]	
20	400	1	2.870	1.686	0	180.00, 0	3.006	3.185
			(2.970)			(0)	(—)	
			[2.986]			[0]	[3.306]	
20	800	2	3.063	1.890	0	180.00, 0	4.002	5.097
			(3.227)			(0)	(—)	
40	0	0	3.319	1.867	53.95	134.74, 40.93	1.128	0.321
			(3.480)			(53.60)	(—)	
			[3.477]			[53.63]	[1.169]	
40	400	0.25	3.531	1.867	45.11	155.70, 29.28	1.394	0.899
			(3.650)			(42.46)	(—)	
			[3.686]			[44.44]	[1.491]	
40	1,600	1	3.899	2.274	14.59	180.00, 21.70	1.980	2.151
			(4.100)			(0)	(—)	
			[4.079]			[0]	[2.167]	
40	3,200	2	4.221	2.611	0	180.00, 9.43	2.627	3.439
			(4.420)			(0)	(—)	
40	4,800	3	4.468	2.863	0	180.00, 6.97	3.202	4.535
			(4.690)			(0)	(—)	
60	0	0	3.991	1.918	59.16	129.38, 44.97	0.890	0.209
			[4.203]			[58.94]	[0.904]	
60	900	0.25	4.2606	2.234	50.27	152.04, 34.31	1.096	0.686
			(4.260)			(50.01)	(—)	
60	3,600	1	4.722	2.730	28.10	180.00, 26.18	1.554	1.704
			(4.912)			(23.29)	(—)	
			[4.941]			[25.37]	[1.699]	
60	5,760	1.60	4.988	3.013	0	180.00, 23.57	1.868	2.359
100	1,000	0.20	5.404	2.767	57.27	142.12, 40.10	0.793	0.416

*Subscript 1: upstream cylinder; subscript 2: downstream cylinder.
**Values in brackets are for single-cylinder situation. ( ): Badr (1984), $Pr = 0.70$. [ ]: present work, $Pr = 0.72$.

for the downstream cylinder. The reason for this behavior is that the increasing Gr causes an increase in flow velocity near the surfaces of the cylinders. It results in a greater $\partial u_t/\partial n$, the gradient of tangential velocity in the direction normal to the surfaces of the cylinders, at the cylinder surface; i.e., a greater surface shear stress. For a higher Gr/Re^2 situation, the velocity near the surface of downstream cylinder is accelerated by the buoyance force created by the both cylinders. Accordingly, the increase of $\partial u_t/\partial n$ at the surface of the downstream cylinder is greater than that of the upstream cylinder. It can be seen from

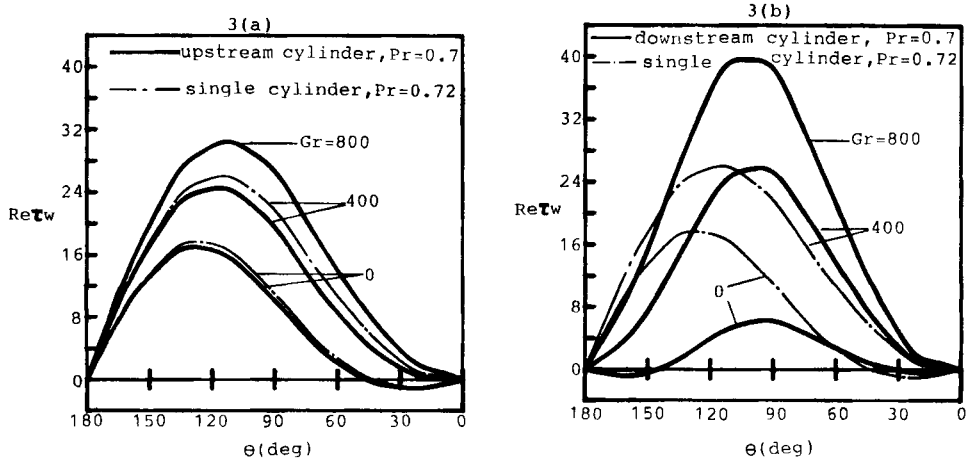

Figure 3. Surface shear stress distribution at $Pr = 0.7$ and $Re = 20$, and comparison with results for a cylinder at $Pr = 0.72$ and $Re = 20$.
(a) Upstream cylinder. (b) Downstream cylinder.

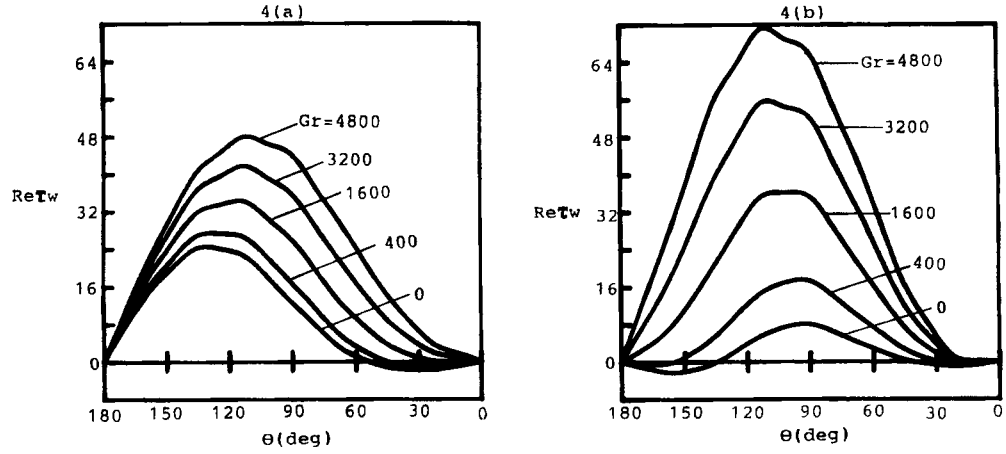

Figure 4. Surface shear stress distribution at Pr = 0.7 and Re = 40.
(a) Upstream cylinder. (b) Downstream cylinder.

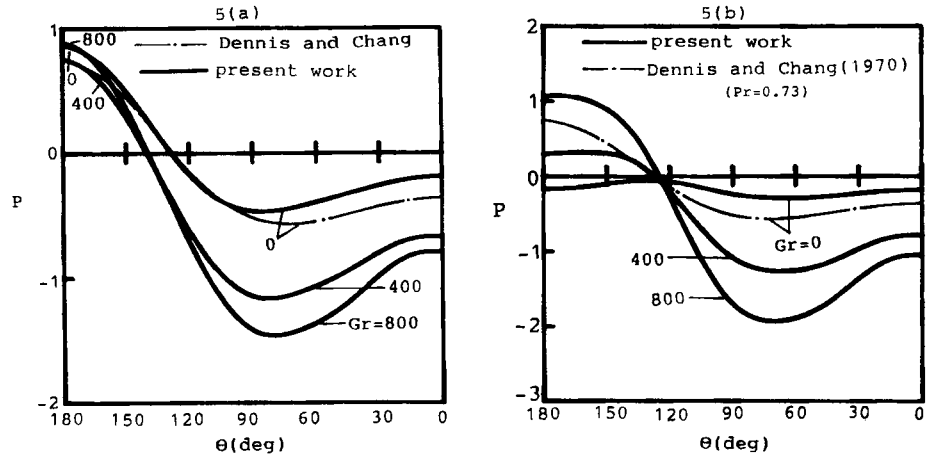

Figure 5. Surface pressure distribution at Pr = 0.7 and Re = 20, and comparison with results of Dennis and Chang (1970) for a cylinder at Pr = 0.73 and Re = 20.
(a) Upstream cylinder. (b) Downstream cylinder.

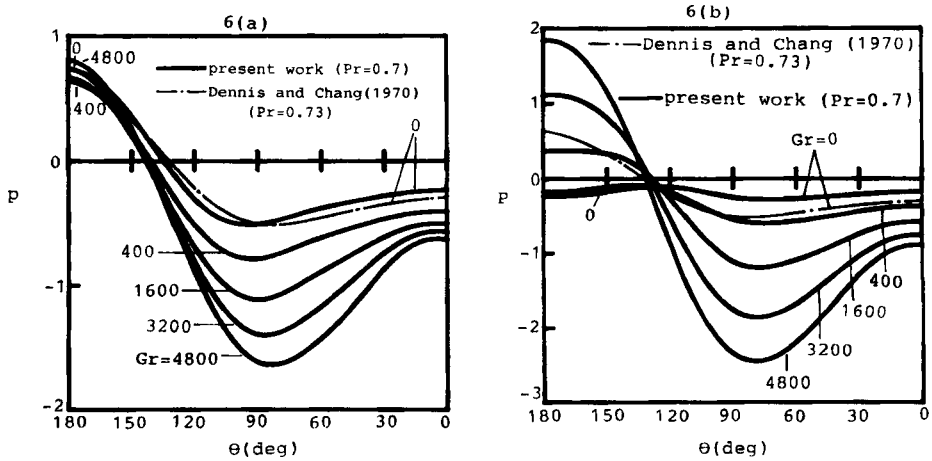

Figure 6. Surface pressure distribution at Pr = 0.7 and Re = 40, and comparison with results of Dennis and Chang (1970) for a cylinder at Pr = 0.73 and Re = 40.
(a) Upstream cylinder. (b) Downstream cylinder.

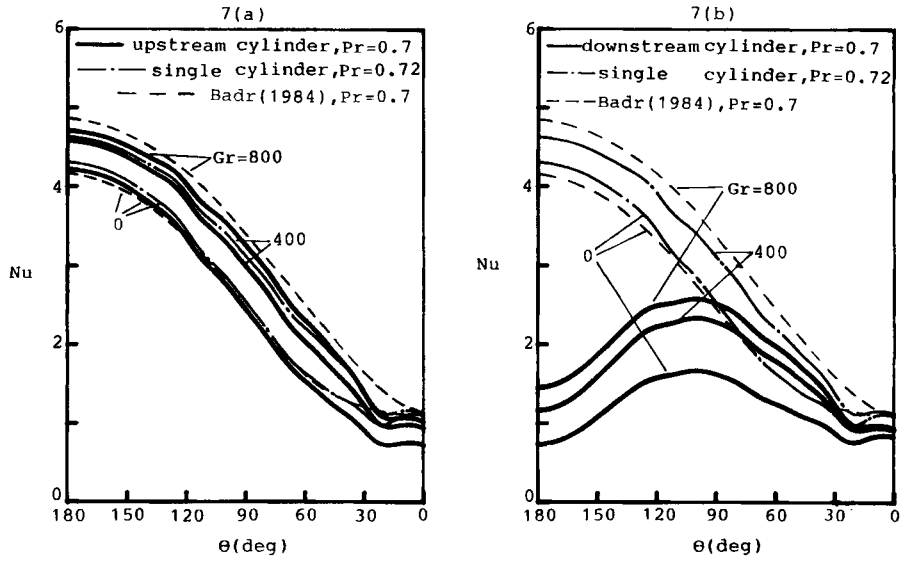

Figure 7. Variation of local Nusselt number at $Pr = 0.7$ and $Re = 20$, and comparison with the results of Badr (1984) for a single cylinder at the same Pr and Re.
(a)Upstream cylinder. (b) Downstream cylinder.

Table 1 that Cf_1, the total friction drag coefficient of upstream cylinder is greater than Cf_2, the total friction drag coefficient of downstream cylinder when $Gr/Re^2 \geq 0.25$. And Cf_1 is less than Cf_2 when $Gr/Re^2 \geq 1.0$. A comparison with the single-cylinder situation at the same Re, but for $Pr = 0.72$ instead of $Pr = 0.7$ considered in the present study. It is shown in Figure 3a that the surface shear stress, $Re\tau_w$, of the upstream cylinder is slightly less than that of the single cylinder. The difference in $Re\tau_w$ between the upstream cylinder and the single cylinder is due to the difference in Pr and the interference produced by the downstream cylinder. And it is shown in Figure 3b that there is a significant difference in $Re\tau_w$ between the downstream cylinder and the single cylinder.

The dimensionless surface pressure distributions at $Re = 20$ and 40 for different values of Gr and a comparison with the forced convective result for a single cylinder obtained by Dennis and Chang (1970) at the same Re but at $Pr = 0.73$ instead of $Pr = 0.70$ considered for the two cylinders in the present investigation are given in Figure 5 and 6, respectively. It can be seen in Figures 5a and 6a that for the upstream cylinder the increasing Gr tends to create a significant decrease in surface pressure near the rear stagnation point ($\theta = 0°$). The response of the surface pressure to the increase in Gr near the front stagnation point ($\theta = 180°$) of the upstream cylinder is slightly different. At first, a small increase in Gr above its zero causes a decrease in P until reaching its minimum value. Further increasing Gr results in increasing P near $\theta = 180°$. Meanwhile, it can be seen in Figures 5a and 6a that the pressure distribution of the upstream cylinder

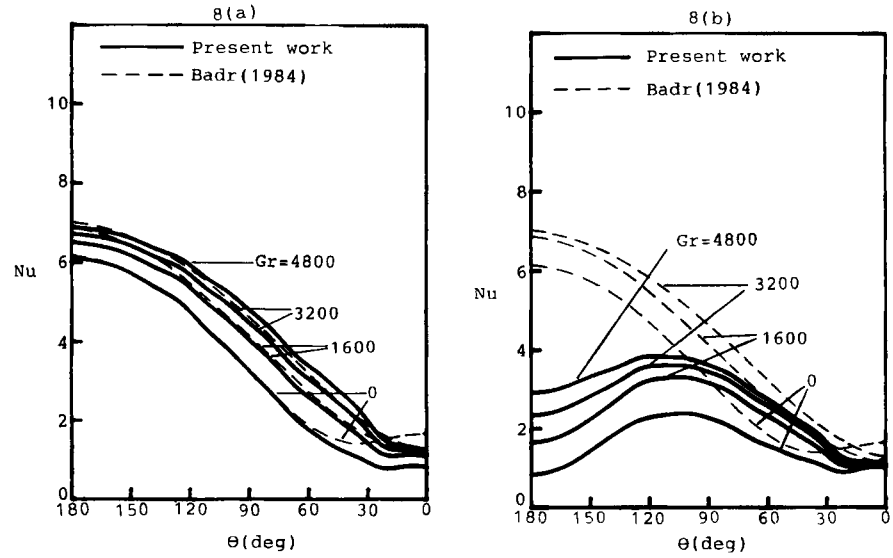

Figure 8. Variation of local Nusselt number at $Pr = 0.7$ and $Re = 40$, and comparison with results of Badr (1984) for a single cylinder at the same Pr and Re.
(a) Upstream cylinder. (b) Downstream cylinder.

is slightly different from that of the single cylinder. It also clear from Figures 5b and 6b that the increasing Gr tends to create a significant increase in P near $\theta = 180°$ and a significant decrease in P near $\theta = 0°$ for the downstream cylinder. And there is a significant difference in P between the downstream cylinder and the single cylinder. Meanwhile, the pressure distribution of the downstream cylinder for the situation of $Gr = 0$ varies slightly from a small value below the line of $P = 0$ shown in Figures 5b and 6b. This phenomenon may be due to the effect of the flow of separation of the upstream cylinder when $Gr = 0$, especially for a high Re situation.

The local Nusselt number distributions at $Re = 20$ and 40 for different values of Gr are given in Figures 7 and 8, respectively. And the results of the two-cylinder situation ($Pr = 0.7$) and the single-cylinder situation ($Pr = 0.72$) of the present study are also compared with those obtained by Badr (1984) ($Pr = 0.70$). It can be seen from Figures 7 and 8 that increasing Gr results in a significant increase in Nu over most of the region of the surfaces of the cylinders except near the rear stagnation point ($\theta = 0°$) of the downstream cylinder and the single cylinder. It shows that the values in Nu of the upstream cylinder are slightly different from those of the single cylinder, but not for the downstream cylinder. It is also clear from Figures 7b and 8b that the maximum values in Nu of the downstream cylinder do not occur at $\theta = 180°$ as do those of the upstream or single cylinder. This phenomenon may be due to the accumulation of the high temperature flow created by the upstream cylinder in the region between the two cylinders. Accordingly, the temperature gradient is reduced (i.e., a reduction in Nu) near $\theta = 180°$ of the downstream cylinder. It results in the significant difference in Nu near $\theta = 180°$ between the downstream cylinder and the single cylinder.

The results are also plotted on the same coordinates used in the studies of Oosthuizen and Madan (1970) and Jackson and Yen (1971), as can be seen in Figure 9. The single curve in Figure 9 suggested by Jackson and Yen (1971) for the single-cylinder situation is the equation $\overline{Nu}/\overline{Nuf} = (1 + Gr/Re^2)^{0.2133}$ where $\overline{Nuf}$ is the average Nusselt number for the forced convection.

It is shown in Figure 9 that the effect of the parameter Gr/Re^2 on the ratio between the average Nusselt numbers of combined and forced convection for the upstream cylinder is close to that of the single cylinder, but not for the downstream cylinder. It can also be seen in Figure 9 that the greater the Re, the greater the effect of Gr/Re^2 on $\overline{Nu}/\overline{Nuf}$ for both cylinders in the tandem arrangement situation.

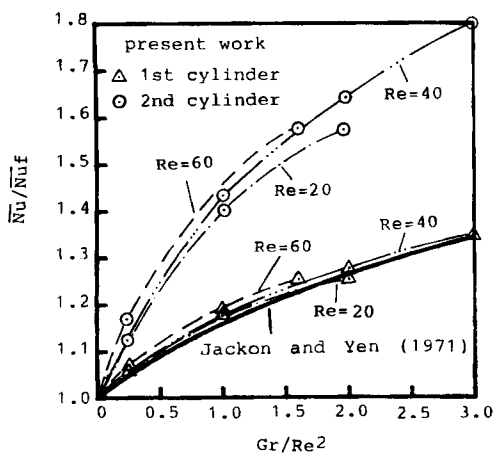

Figure 9. Effect of parameter Gr/Re^2 on the ratio between the average Nusselt number, $\overline{Nu}$, of combined convection and $\overline{Nuf}$, of forced convection.

Notation

$\tilde{A}$ = global coefficient matrix
A^e = area of single element
$\tilde{A}^e$ = coefficient matrix of single element
a_{ij} = element of global coefficient matrix
$\tilde{B}$ = natural boundary condition vector
b_j = element of natural boundary conditon vector
C = specific heat
C_{ij} = element of coefficient matrix of single element
C_f = friction drag coefficient
Gr = Grashof number, $8g\beta(Tw - T\infty)\,Ro^3/\nu^2$
g = gravitational acceleration
h = local heat transfer coefficient
K = thermal conductivity
N_i = shape function
$Nu, \overline{Nu}$ = local and average Nusselt numbers
P = dimensionless pressure, $(P^* - P\infty)/\rho u_\infty^2$
$P^*, P\infty$ = Pressure, free stream pressure
Pe = Peclet number, $RePr$
Pr = Prandtl number, $\mu c/K$
Ra = Rayleigh number, $GrPr$
Re = Reynolds number, $2Rou\infty/\nu$
Ro = radius of cylinder
T = temperature
Tw = temperature on cylinder surface with fixed value
$T\infty$ = free stream temperature
u = dimensionless x direction component of velocity, $u^*/u\infty$
u^* = x direction component of velocity
$u\infty$ = free stream velocity
v = dimensionless y direction component of velocity, $v^*/u\infty$
v^* = y direction component of velocity
X = x direction axis
x = dimensionless x direction coordinate, $x^*/2Ro$
x^* = x direction coordinate
Y = y direction axis
y = dimensionless y direction coordinate, $y^*/2Ro$
y^* = y direction coordinate

Greek letters

β = coefficient of volumetric thermal expansion
Γ = boundary of flow domain
Γ_1 = boundary with fixed value boundary condition
Γ_2 = boundary with natural boundary condition
θ = plane angle
$\tilde{\lambda}$ = primitive variable vector
μ = dynamic viscosity
ν = kinematic viscosity, μ/ρ
ρ = density of fluid
τ_w = dimensionless surface shear stress, $\tau_w^*/\rho\mu_\infty^2$
τ_w^* = surface shear stress
ϕ = dimensionless temperature, $(T - T\infty)/(T_w - T\infty)$
Ω = flow domain of total elements
Ω_e = flow domain of single element

Literature Cited

Arie, M., et al., "Pressure Fluctuations on the Surface of Two Circular Cylinders in Tandem Arrangement," *J. Fluids Eng., Trans. ASME*, **105**, 161 (1983).

Badr, H. N., "Laminar Combined Convection from a Horizontal Cylinder—Parallel and Contra Flow Regimes," *Int. J. Heat Mass Transfer*, 27(1), 15 (1984).

Dennis, S. C. R., and G. Chang, "Numerical Solution for Steaty Flow

Past a Circular Cylinder at Reynolds Number up to 100," *J. Fluid Mech.*, **42,** 471 (1970).
Hatton, A. P., D. D. James, and H. W. Swire, "Combined Forced and Natural Convection with Low-Speed Air Flow over Horizontal Cylinder," *J. Fluid Mech.*, **42,** 17 (1970).
Hood, P., "Frontal Solution Program for Unsymmetric Matrices," *Int. J. Num. Meth. Eng.*, **10,** 379 (1976).
Irons, B. M., "A Frontal Solution Program for Finite Element Analysis," *Int. J. Num. Meth. Eng.*, **2,** 5 (1970).
Igarashi, T., "Flow Characteristics around Two Circular Cylinders in Tandem Arrangement. I," *Trans. JSME*, **46** (406), 1026 (1980).
Jackson, T. W., and H. H. Yen, "Combined Forced and Free Convective Equation to Represent Combined Heat Transfer Coefficients for Horizontal Cylinders," *J. Heat Transfer*, **93,** 247 (1971).
Joshi, N. D., and S. P. Sukhatme, "An Analysis of Combined Free and Forced Convection Heat Transfer from a Horizontal Circular Cylinder to a Transverse Flow," *J. Heat Transfer*, **93,** 441 (1971).
Merkin, J. H., "Mixed Convection from a Horizontal Circular Cylinder," *Int. J. Heat Mass Transfer*, **20,** 73 (1976).
Oosthuizen, P. H., and S. Madan, "Combined Convection Heat Transfer from Horizontal Cylinders in Air," *J. Heat Transfer*, **92,** 194 (1970).
Sparrow, E. M., and L. Lee, "Analysis of Mixed Convection about a Horizontal Cylinder," *Int. J. Heat Mass Transfer*, **19,** 229 (1976).
Taylor, C., and T. G. Hughes, *Finite Element Programming of the Navier-Stokes Equations*, Pineridge Press, West Cross, Swansea, England, 30 (1981).

Manuscript received Feb. 21, 1985, and revision received June 4, 1985.